REPORT DOCUMENTATION PAGE

Form Approved
OMB No. 0704-0188

1. AGENCY USE ONLY *(Leave blank)*	2. REPORT DATE	3. REPORT TYPE AND DATES COVERED
	10 Oct 97	Interim Progress, 1 Sept 96-1 Sept 97

4. TITLE AND SUBTITLE

Improved Sampled Grating DBR Widely-Tunable 1.55μm Lasers

5. FUNDING NUMBERS

(c) N00014-96-1-6014

6. AUTHORS

Larry A. Coldren & Beck Mason

7. PERFORMING ORGANIZATION NAME(S) AND ADDRESS(ES)

University of California
Department of ECE
Santa Barbara, CA 93106

8. PERFORMING ORGANIZATION REPORT NUMBER

9. SPONSORING/MONITORING AGENCY NAME(S) AND ADDRESS(ES)

Department of the Navy
Naval Research Laboratory
4555 Overlook Avenue, SW
Washington DC 20375-5326

10. SPONSORING/MONITORING AGENCY REPORT NUMBER

11. SUPPLEMENTARY NOTES

12a. DISTRIBUTION/AVAILABILITY STATEMENT

Approved for public release; distribution unlimited.

12b. DISTRIBUTION CODE

13. ABSTRACT *(Maximum 200 words)*

The objective of this program is to develop a widely tunable semiconductor laser diode with an integrated wavelength monitor. The technology development necessary for achieving this goal has been broken down into five separate tasks. These are being pursued in a three year research program. This report documents the progress that has been made in the first year of this program. Advancement has been made in four separate areas; development of a four electrode ridge SGDBR (Task 1), optimization of the waveguide design for high index shift (Task 2), design of a buried heterostructure SGDBR (Task 3), and research on an integrated wavelength monitor.

14. SUBJECT TERMS

15. NUMBER OF PAGES

8

16. PRICE CODE

17. SECURITY CLASSIFICATION OF REPORT	18. SECURITY CLASSIFICATION OF THIS PAGE	19. SECURITY CLASSIFICATION OF ABSTRACT	20. LIMITATION OF ABSTRACT
unclassified	unclassified	unclassified	UL

Annual Progress Report NRL Project for "Improved Sampled Grating DBR Widely-Tunable 1.55μm Lasers"

The objective of this program is to develop a widely tunable semiconductor laser diode with an integrated wavelength monitor. The technology development necessary for achieving this goal has been broken down into five separate tasks. These are being pursued in a three year research program. This report documents the progress that has been made in the first year of this program. Advancement has been made in four separate areas; development of a four electrode ridge SGDBR (Task 1), optimization of the waveguide design for high index shift (Task 2), design of a buried heterostructure SGDBR (Task 3), and research on an integrated wavelength monitor.

Task 1. Four Electrode SGDBR

The objective of this task is to design and fabricate a SGDBR with full wavelength coverage over 35 nm. The device design employs periodically sampled grating mirrors which have multiple reflection peaks spaced approximately 5 nm apart. The duty cycle and sampling periods have been optimized for the desired wavelength coverage. A phase control section was added to the laser to enable alignment of the cavity mode with the mirror reflection peaks. The device was fabricated using a ridge waveguide process with passive regions formed by a combination of etching and MOCVD regrowth.

Devices were made with 4, 5 and 6 μm ridge widths and 2 different mirror structures. The active region length was 550μm long, with a 150μm long phase control section and 500 and 750μm long front and back mirrors. The asymmetric mirror lengths provide both narrower spectral width and higher output power. The different ridge widths were fabricated to determine the best size for optimum device performance. Simulations predicted that the wider ridge widths would increase the overlap between the injected carriers and the optical mode for enhanced tuning.

The L-I characteristics were measured for 25 devices at each of the different ridge widths. Using this data the average threshold current and differential efficiency were calculated for each size. These are shown in Fig. 1a. Fitting a theoretical curve to this data indicates that the optimum width for minimum threshold will be below 4 μm. Fig. 1b shows the differential efficiency as a function of ridge width. This indicates an increase in η_d as we move to narrower ridges. Tuning tests on devices of all three dimensions showed no correlation between ridge width and tuning current. In fact the smaller devices had better tuning characteristics. Based on these results, the design of the ridge waveguide SGDBR, with the integrated wavelength monitor employs 3μm wide ridges.

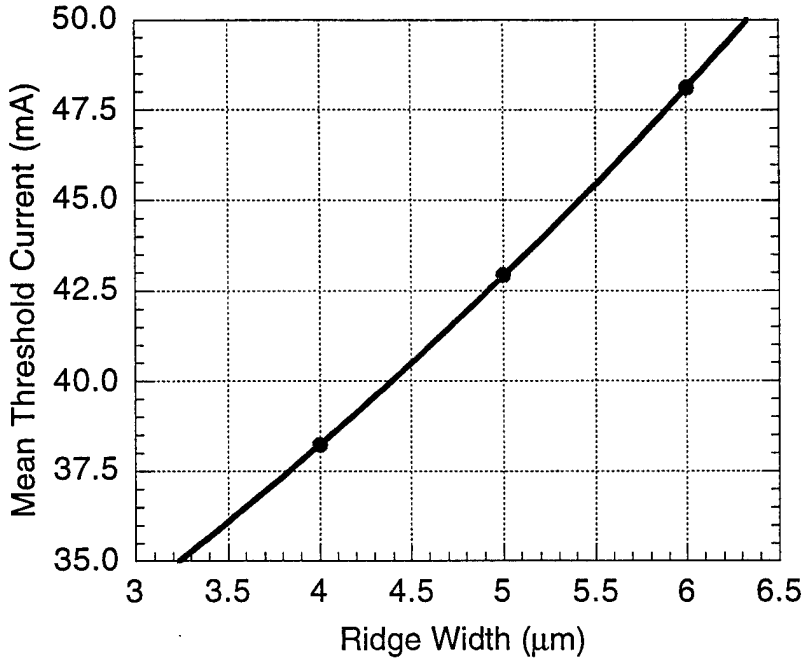

Figure 1a Threshold vs. Device Width

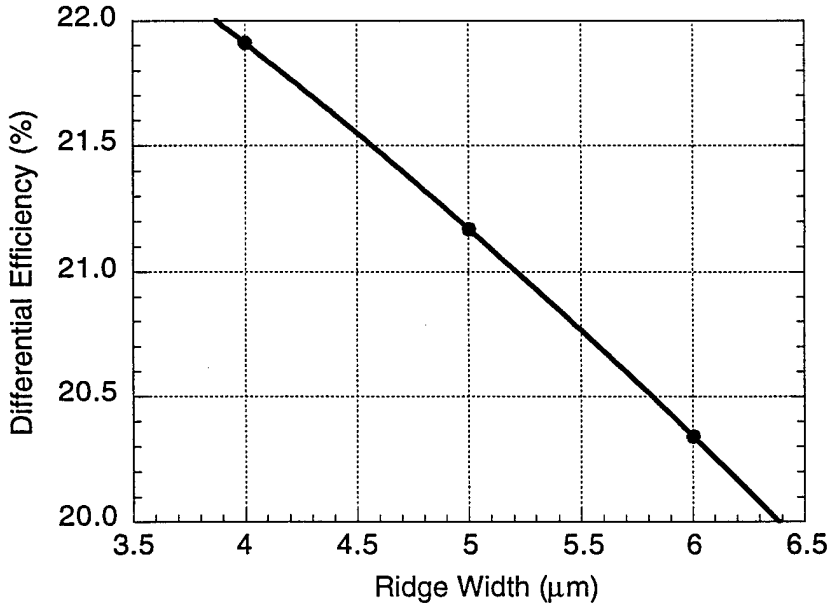

Figure 1b Differential Efficiency vs. Device Width

Two key improvements over previous devices have been implemented in this task. An improved active region with higher peak gain and lower leakage current has been developed. The active region consists of four 1% compressive strained quaternary quantum wells grown on top of the waveguide. The performance was characterized by growing a conventional laser structure and fabricating broad area devices. The results from these lasers indicated an injection efficiency η_i of 72.5%, internal loss α_i of 12 cm^{-1}, and a threshold current density of 280 A/cm^2 for a 2 mm long device. With a value for the modal gain coefficient Γg_o of 33 cm^{-1}.

The other improvement is the addition of a phase control region to the cavity. The phase control section is used to align the cavity mode with the mirror reflection peaks. This reduces the mirror loss and improves the power stability throughout the tuning range. The output power and wavelength dependence on the current in the phase section is shown in Fig. 2. As the mode is detuned from the mirror peak the output power and the side mode suppression ratio decreases.

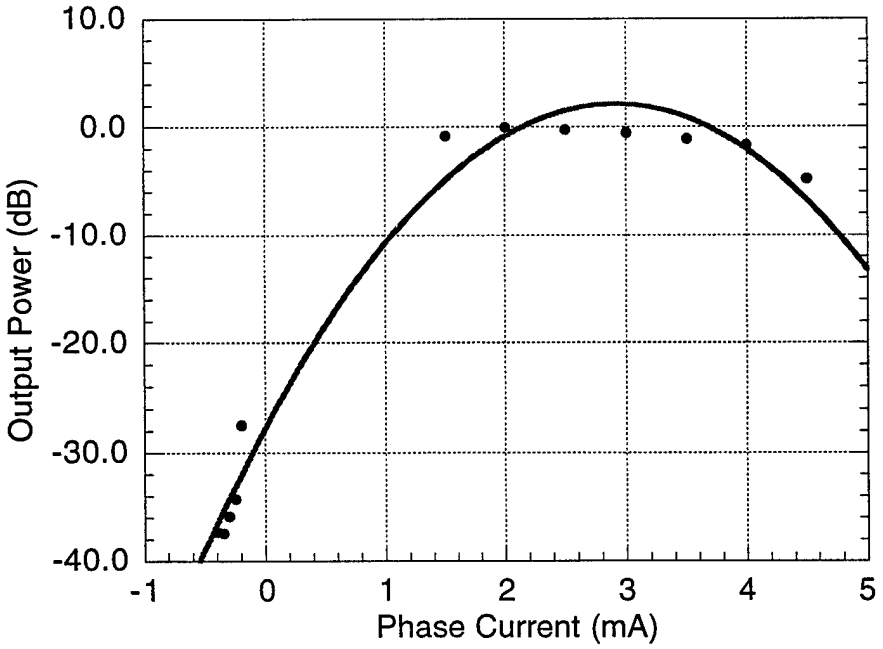

Figure 2. Phase Section Detuning Response

The mirror structures for the four section devices included two different designs. The first has mirror peak separations of 4 and 4.5 nm, which gives it a maximum theoretical tuning range of 36 nm using 8 reflection peaks. The second design has spacings of 4.5 and 5 nm yielding a slightly longer tuning range of 45 nm. The coarse tuning results from one of the 36 nm tuning range devices are shown in Fig. 3a,b. The minimum mirror tuning

required to achieve full wavelength coverage is equal to the maximum comb spacing. The objective is to scale the design up to a theoretical tuning range of greater than 65 nm. In this design we have attempted to optimize the tradeoff between the side mode suppression ratio and the maximum tuning range. For the longer tuning range designs the mirror reflection peaks will be narrower due to the increased number of sampling periods. This will improve the side mode suppression for these devices.

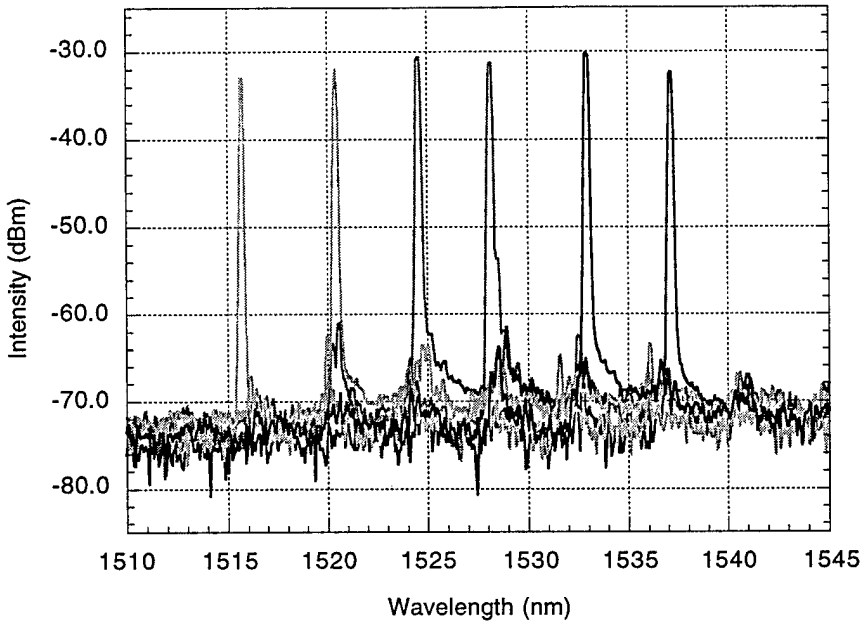

Figure 3a. Lasing Spectra

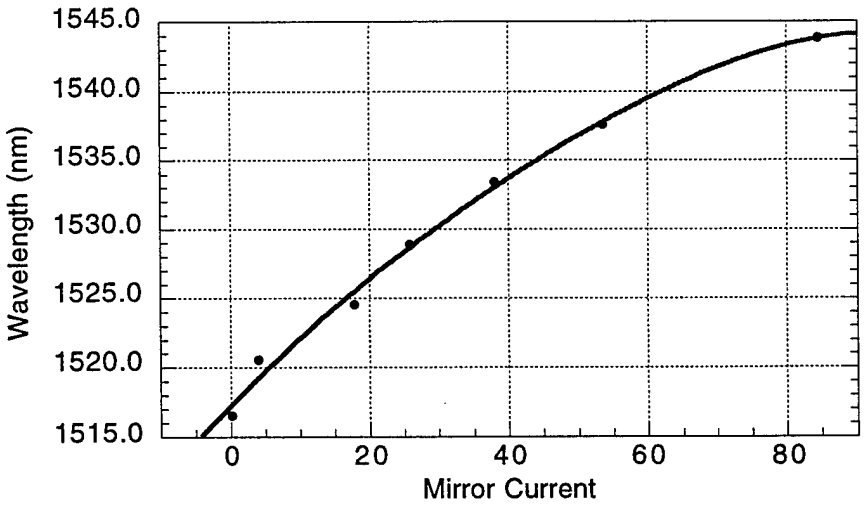

Figure 3b. Coarse Tuning Curve

Unfortunately these devices were not capable of achieving continuous wavelength coverage over the entire tuning range. Their fine tuning was limited to 2.5 nm which is about half of what is required. The tuning range is being limited by thermal compensation of the carrier induced index shift. This is indicative of high leakage currents and poor carrier confinement in the device. Using a buried heterostructure will improve the carrier confinement. We are also investigated a dry etch process for fabricating the gratings. This process will enable an InP surface to be maintained over the waveguide for the regrowth. This will improve the quality of the regrowth interface and reduce the contribution to leakage current from non-radiative recombination at the interface.

Task 2. Optimized Waveguide Design

The previous SGDBR structure employed a quaternary waveguide with a band gap wavelength of 1.3 μm (1.3Q). The amount of index shift that can be achieved by carrier injection into the waveguide increases as bandgap of the material is reduced. The loss associated with the waveguide will also increase as the bandgap is reduced. Both of these effects are highly nonlinear and depend on the wavelength of the laser. The optimum composition for the highest ratio of index change to absorption increase for light at 1.55 μm is a quaternary material with a band gap wavelength around 1.4 μm.

The first set of four section devices have a 1.35Q waveguide with a single 200 Å stop etch layer between that and the quantum wells (Fig. 4a). The gratings are etched directly into the waveguide layer, which thins it, increasing the active passive junction discontinuity. Reflections from this interface are minimized by using a laterally tapered junction.

Creating active passive junctions that result in a large amount of exposed quaternary material on the surface poses a problem for efficient MOCVD regrowth. During the heat up phase of the growth cycle the surface is maintained by a flow of column V source material over the surface of the wafer. The quality of the regrowth interface is extremely sensitive to this purge and the composition of the gas stream must be optimized for each type of material. When both InP and quaternary material are exposed it is necessary to purge with tertiarybutylphosphine (TBP) only and the purge cycle must be shortened in order to protect the surface. The shorter purge times and unoptimized flow conditions result in a higher defect density in the regrowth and lower interface quality. The new device design has a separate grating layer on top of the waveguide. A thin InP layer over it remains when the active region is removed by a selective wet etch. The gratings are then formed by a methane hydrogen argon, dry etch process with the waveguide protected by a SiNx mask. This allows higher kappa gratings to be produced with more precise control. It also facilitates the MOCVD regrowth since 95% of the surface area is now InP. Longer purge times with TBP overpressure can be used resulting in better regrowth quality.

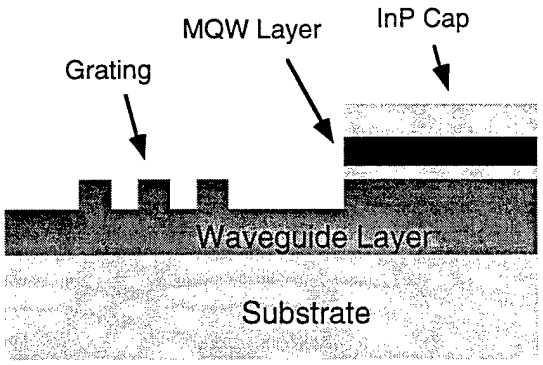

Fig. 4a. Old device structure

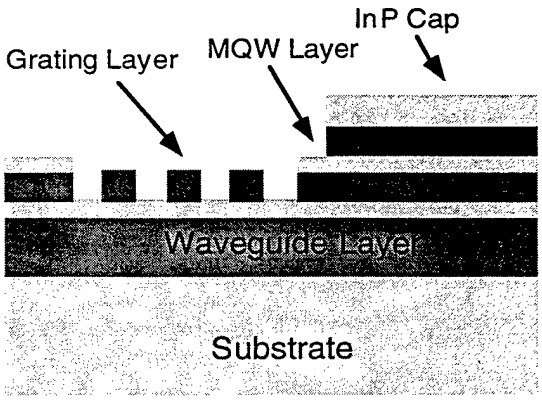

Fig. 4b. New device structure

The improved regrowth quality which can be achieved with the structure shown in figure 4b is demonstrated in Fig. 5. Both samples were from the same base structure growth and both had identical regrowth preparation. Sample a is typical of the regrowth quality when exposed quaternary material covers close to 70% of the surface. Sample b shows considerably better quality regrowth resulting from the longer purge time in TBP and the reduction in exposed quaternary material.

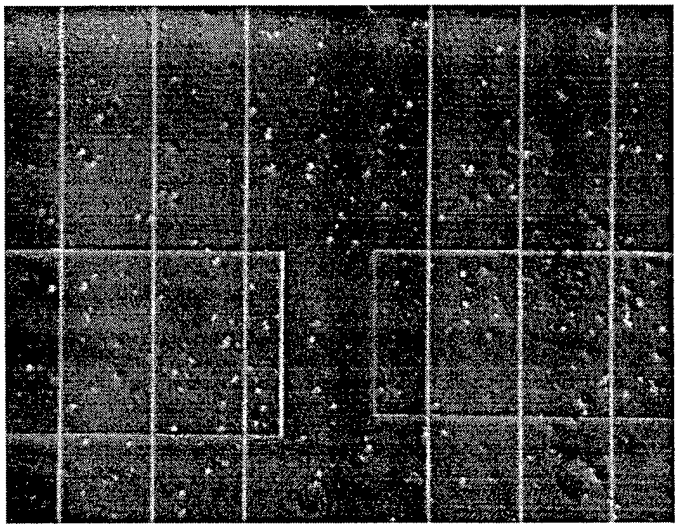

Fig. 5a. Old device structure

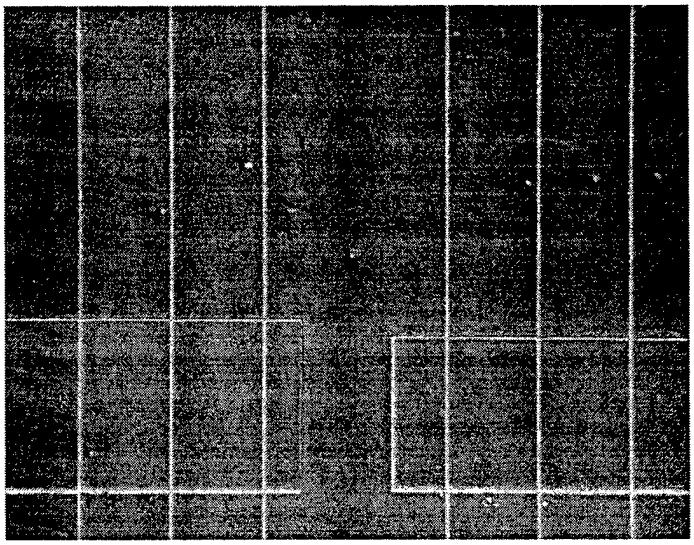

Fig. 5b. New device structure

Task 3. Buried Heterostructure

The major focus of this task is to develop a buried heterostructure design for the SGDBR. This phase of the research program is the most growth intensive area. In the buried heterostructure device, the active region is clad on either side by higher band gap material which blocks lateral carrier leakage. A buried heterostructure will provide improved carrier confinement both in the active and passive sections. It is more difficult to fabricate buried devices using MOCVD regrowth because of the plane selectivity of the growth rate and the dopant incorporation. There are several different types of blocking structures which can be used for MOCVD buried regrowth. The simplest method is to etch a ridge cutting through the quantum wells and the waveguide layer and then regrow p-type InP over the entire structure with an InGaAs cap. The area around the laser is then proton implanted to minimize the leakage current. This is the simplest method and can be effective for low to moderate injection currents. At higher carrier densities, the pn junction which shunts the device, will turn on and the leakage current will increase. A more efficient junction type is a pn-blocking junction. This utilizes alternate n and p doped layers to create a reversed biased junction that blocks carrier leakage. This structure is more difficult to grow, but provides better performance. The other alternative is the Fe-n-p structure. This is in improvement on the pn blocking junction which prevents carriers from shunting around the blocking junction and turning it on. It has similar characteristics to pn blocking structures with improved high speed modulation response.

We fabricated devices with pn blocking layers using a three regrowth process. First, the active passive junction was formed with the gratings. This was regrown with a 5000 Å

InP cap layer. A ridge was then etched using a SBW etchant and a SiNx mask. The mask was left on and the blocking structure was regrown around the device. Then the mask was removed and a final cap layer grown. A stain etched SEM-image of the device is shown in Fig. 6. These devices did not lase. They exhibited high leakage currents most likely due to the poor regrowth interface and the low doping in the n-type blocking layer. We plan to repeat this process with optimized doping levels and an improved regrowth process. The base structure has been grown for this, and the first regrowth has been completed. We also plan to attempt the simpler p-type regrowth with implant process as well as a full blocking junction design.

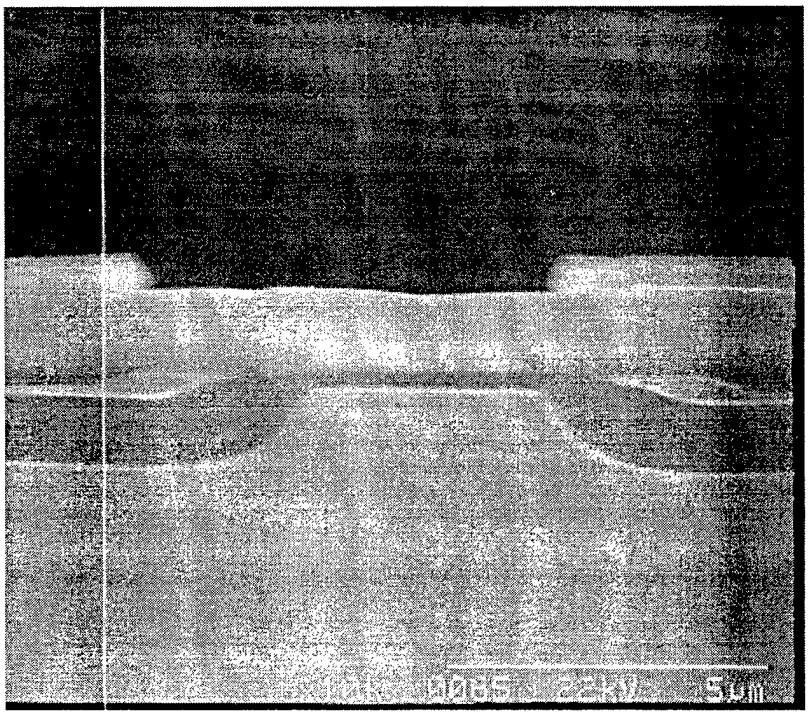

Fig 6. SEM of Buried Heterostructure SGDBR

Integrated Wavelength Monitoring

This area of the project evolved out of the requirement for simple "two knob" operation of the SGDBR one for amplitude and the other for wavelength. The complexity of the tuning mechanism in these types of lasers makes it desirable to have an integrated method for providing wavelength monitoring. This would operate in much the same way that the backside photodetector provides output power monitoring in a conventional laser diode. There are many different methods for achieving a wavelength dependent signal in an integrated photonic circuit. We focused on a design that would provide a compact, robust wavelength monitor that could easily be integrated with the existing device process. The design is based on a two mode interference waveguide. Using the difference in the propagation velocity for the lowest order odd and even modes in an asymmetrically

excited waveguide, a wavelength dependent output signal can be generated. The design was simulated and refined using the beam propagation method. This design can be integrated with the existing laser process and provides a monotonicly varying output signal over a wide wavelength range. Ultimately, the sensitivity of the structure will be limited by the signal to noise ratio of the detectors. Since the waveguide is integrated directly with the laser, it is expected that the high optical signal levels will provide a clean output signal.

Light is launched off axis into the TMI waveguide and propagates along it. At the output, the splitting ratio into the two guides is governed by the phase difference between the excited waveguide modes which is wavelength dependent. The output range is governed by the device length. For a 100 nm range the device length is ~2 mm which is large compared to conventional laser diodes, but much smaller than an AWG or Mach-Zehnder based device would be. Fabrication of ridge waveguide wavelength monitors integrated with SGDBR lasers is nearing completion at this time and test results are expected soon.